Effects of 3G cell phone exposure on the structure and function of the human cytochrome P450 reductase

Shazia Tanvir, György Thuróczy, Brahim Selmaoui, Viviane Silva Pires Antonietti, Pascal Sonnet, Delia Arnaud-Cormos, Philippe Lévêque, Sylviane Pulvin, René De Seze

Effects of 3G Cell Phone Exposure on the Structure and Function of the Human Cytochrome P450 Reductase

Shazia Tanvir [1], György Thuróczy [2,3], Brahim Selmaoui [2,3], Viviane Silva Pires-Antonietti [4], Pascal Sonnet [4], Delia Arnaud-Cormos [5], Philippe Lévêque [5], Sylviane Pulvin [1] and René de Seze [2,3]

[1] Sorbonne Universités, Université de Technologie de Compiègne, Laboratoire de Génie Enzymatique et Cellulaire, FRE CNRS 3580, CS60319, 60203 Compiègne Cedex. France

[2] Unité de toxicologie expérimentale TOXI-PériTox UMR-I 01
Institut National de l'Environnement Industriel et des RISques (INERIS)
Parc ALATA BP2, 60 550 Verneuil-en-Halatte, France

[3] PériTOX, UPJV, Faculté de Médecine – 80 000 Amiens, France

[4] Université de Picardie Jules Verne, Laboratoire de Glycochimie, des Antimicrobiens et des Agroressources, UMR CNRS 7378, UFR de Pharmacie, 80 037, Amiens, France

[5] Université de Limoges, CNRS, XLIM, UMR 7252, F-87000 Limoges, France

*Running title: Effects of Cell Phone Exposure on Cytochrome P450 Reductase

Correspondence should be addressed to: René de Seze, TOXI, INERIS, Parc ALATA BP2, Verneuil-en-Halatte, 60 550 France, Tel.: +33-344556594; Fax: +33-344556767; E-mail: rene.de-seze@ineris.fr

Abstract

Cell phones increase exposure to radiofrequency (RF[1]) electromagnetic fields (EMFs). Whether EMFs exert specific effects on biological systems remains debatable. This study investigated the effect of cell phone exposure on the structure and function of human NADPH-cytochrome P450 reductase (CPR). CPR plays a key role in the electron transfer to cytochrome P450, which takes part in a wide range of oxidative metabolic reactions in various organisms from microbes to humans. Human CPR was exposed for 60 minutes to 1966-MHz RF inside a transverse electromagnetic cell (TEM-cell) placed in an incubator. The specific absorption rate (SAR) was 5 $W.kg^{-1}$. Conformation changes have been detected through fluorescent spectroscopy of flavin and tryptophan residues, and investigated through circular dichroism, dynamic light scattering and microelectrophoresis. These showed that CPR was narrowed. By using cytochrome C reductase activity to assess the electron flux through the CPR, the Michaelis Menten constant (Km) and the maximum initial velocity (Vmax) decreased by 22% as compared with controls. This change was due to small changes in the tertiary and secondary structures of the protein at 37◦C. The relevance of these findings to an actual RF exposure scenario demands further biochemical and in-vivo confirmation.

Keywords: Cell phone radiofrequency; cytochrome P450 reductase; circular dichroism; fluorescence spectroscopy; zeta potential; dynamic light scattering

[1] The abbreviations used are: RF, radiofrequency; CPR, cytochrome P450 reductase; EMFs, electromagnetic fields; DLS, dynamic light scattering; 3G, 3rd generation of mobile telephony; TEM-cell, transverse electromagnetic cell; SAR, specific absorption rate; GSM, global system for mobile telephony; WCDMA, wideband code division multiple access; Universal Mobile Telecommunication System (UMTS); FDTD, Finite Difference-Time Domain; Trp, tryptophan

Introduction

Cellular telecommunication is inseparable from our everyday life. Numerous studies have investigated the potential impact of Global System for Mobile Communication (GSM) on biological systems with several positive and negative outcomes. The biological effects of RF exposure may interact at different levels of biological systems such as at the organic, tissue, cellular and macromolecular level. It is reasonable to assume that any possible biological damage could start at a molecular level involving biological macromolecules. It has been suggested that the main target of RF could be cell membranes and proteins (channel proteins, signal transducers, etc.) or enzymatic complexes located within membranes [1]. However, few investigations have reported as to the possible subcellular effects of RF exposure emitted by 3G cell phones. Proteins are macromolecules found in a living cell and play a crucial role in almost every biological process.

One first step and simplified way is to study the direct effect of RF exposure on protein conformation and function. Some studies suggest that non-thermal microwave exposures could alter protein expression and/or induce conformational changes [2, 3]. In these macromolecules, charge distribution may be the cause or the consequence of a conformation change and functional modification of the biological activity could result therefrom. [4-6]. Among such enzymatic complexes, embedded in biological membranes and potentially affected by EMF are cytochrome P450 dependent monooxygenases as well as enzymatic proteins (NADH cytochrome b5, b5 reductase). The above complexes are the key enzymes of phase I reactions, which initiate the metabolism of lipid soluble xenobiotics [7]. Some physiological effects attributable to RF radiation may eventually be traced to alterations in cell membrane function. As it is involved in electron transportation to cytochrome P450, the human NADPH-CPR is suitable as a model for intensive investigation.

In order to better understand the biological effects of RF, different techniques like fluorescence, circular dichroism (CD), dynamic light scattering (DLS) and microelectrophoresis can be used to investigate possible RF-induced modifications. Many biological molecules absorb photons, but few fluoresce, particularly among aromatic amino acids. Two of the most important types of biomolecules that do fluoresce (i.e., those which have proved useful in analytical procedures) are tryptophan and flavins (FAD and FMN) [8]. Both of these intrinsic fluorescence markers are present in the NADPH-cytochrome P450 reductase, allowing the examination of structural changes which take place in this protein after exposure. For these reasons, we chose to study the effects of RF EMF on human CPR. Human CPR is a complex multi-domain membrane-bound diflavo-protein and a key electron donor to P450-mediated microsomal electron transport system. As underlined by Wang et al. [9], microsomal electron transport mediated by cytochrome P450 is responsible for oxidative metabolism of both endogenous and exogenous compounds. Electron transport is mediated by a multicomponent monooxygenase system, in which reducing equivalents of NADPH are in fine transferred to molecular oxygen [10, 11]. A simple form of the monooxygenase system consists of CPR and one of many cytochrome P450 isozymes [12, 13]. Both CPR and microsomal cytochromes P450 are integral membrane proteins; together with CPR, the only other mammalian enzyme containing both FMN and FAD as prosthetic groups is nitric-oxide synthase and various isoforms thereof. Other physiological electron acceptors of CPR include microsomal heme oxygenase [14], cytochrome b5 [15] and, although not used in normal physiological reactions, CPR is capable of transferring reducing equivalents to cytochrome c [16]. As only two protein components are required to catalyze the hydroxylation of a number of substrates, this system represents a simple model for other more complex electron transport systems.

Fluorescence spectroscopy reveals microstructural details of a chromophore's environment at very low chromophore concentrations. The fluorescence properties of proteins are highly individual, a sort of fingerprint of the protein's structure, and their behavior is largely dependent on folding or unfolding. The CPR molecule is composed of four structural domains: (from the N- to C- termini) the FMN-binding domain, the connecting domain, and the FAD- and NADPH-binding domains. CPR contains two flavin domains (FAD and FMN) and 9 tryptophan residues as internal fluorescence probes. Electrical charges are differently distributed in all macromolecules. For many biomolecules such as proteins, electrostatic

interactions influence their conformations and functions. Several studies demonstrate that hydrodynamic radius and zeta potential can provide information about the change in conformation and surface modification of the biomolecules and particles in solution [17-19]. Since the protein retains its folded conformation, hydrodynamic size and zeta potential (charge) will vary with protein conformation. These parameters can be measured by DLS.

The purpose of the present investigation was, therefore, to determine if exposure to RF signals used by 3G cell phones could alter the structure and activity of CPR.

Materials and methods

2.1 Reagents and chemicals - Highly purified detergent solubilized human CPR was purchased from Sigma-Aldrich (St. Louis, MO, USA). CPR was expressed in baculovirus infected cells containing human cDNA. Its molecular mass was ~78.2 kDa, (95% purity by affinity chromatography). CPR was diluted in 100 mM potassium phosphate buffer, filtered to clear off large sized aggregates and subjected to protein content determination by Modified Lowry assay. 3-ml samplings were poured into a (12.5x12.5x45 mm) polymethylmetacrylate (PMMA) cuvette (VWR, Fontenay-sous-Bois, France) for RF exposure and spectrometric analyses. Horse heart cytochrome C was also purchased from Sigma. Purified water with a typical resistivity of 18 MΩ.cm was produced from a Milli-Q purification system (Millipore, Les Ulis, France). All other reagents were of analytical quality, and all aqueous solutions were prepared with Milli-Q water with a Millipore water purification system.

2.2 RF exposure system - Exposures were carried out in a small TEM-cell placed in a temperature-controlled incubator (Schematic 1**Error! Reference source not found.**). The TEM-cell, designed and built by the XLIM Research Institute (CNRS-University of Limoges, France), is an open RF chamber where the intensity of the exposure inside the chamber depends on the input and reflected RF powers of the system [20-22]. To minimize the reflection of the RF power, the TEM cell was loaded with a 50-ohm load (HTF-525-NM, Trilithic Inc. USA). 3G cell phones use wideband code division multiple access (WCDMA) standard RF signals, also called Universal Mobile Telecommunication System (UMTS), which operate in the frequency range of 1920 to 2170 MHz. The WCDMA modulation is a non-periodic cocktail of signals with 5-MHz bandwidth. The 1966 MHz RF signal modulated by a specific WCDMA signal "cocktail" was generated by a Generic UMTS Signal generator (GUS-6960, Universität Wuppertal, Germany). As the output power level of the generator is limited, a RF power amplifier (OPHIR, 5303069, USA) was connected to guarantee the necessary RF power. A built-in step attenuator of the UMTS generator controlled the exposure level of the sample. The absorbed RF power or SAR in the sample depends on the RF exposure intensity. A polymethylmetacrylate cuvette (4.5 ml, Brand ®, Wertheim, Germany) containing 3 ml of 130 nM CPR was placed in the center position of the TEM-cell and exposed to a 1966 MHz RF signal (Figure 1 (A)). The temperature of the incubator (Certomat HK, France) was controlled within ± 0.5°C during the study. The temperature of the samples inside the cuvette under RF exposure was measured by non-perturbing optical temperature probes (Luxtron model 790, Lumasense, USA). The non-perturbing feature of thermal probes is very important in RF studies. Any metallic wire can enhance the local SAR in the sample. Therefore, during RF exposure, metallic wires must be avoided.

Experimental RF dosimetry - The SAR of the solution was determined experimentally by temperature measurements [20, 23]. The classic method of experimental SAR measurement is based on RF energy absorption in the water solution to produce a rise in temperature. The SAR is linear with the initial slope of the temperature increase. Therefore, the SAR was calculated from the temperature rise produced by short RF exposure according to the equation:

$$SAR\left(W.kg^{-1}\right) = C.\left(dT/dt\right) \quad \textbf{(1)}$$

where dT is the temperature rise in K, dt is the duration of RF exposure in seconds and C is the specific heat of the solution (C = 4187 J.kg^{-1}.K^{-1}). The SAR measurement was performed at the highest RF input power level available in the system to achieve a great enough temperature increase during a short RF

exposure duration. For SAR measurements, the RF input power of the TEM-cell was 3.88 W. The incident and reflected RF powers were monitored by a power meter system with a built-in directional coupler (Rohde-Schwarz FSH-Z44, Germany). The temperature rise in the solution was measured by fiber-optic non-perturbing temperature probes. The non-perturbing fiber-optic probe was inserted into 3 ml of solution at the cuvette cross section center at different heights from the bottom plate. The SAR was calculated by the temperature rise following 30 s of RF exposure from several measurements.

The SAR in the solution was measured at 4, 8, 12, 16, 20 and 24 mm from the bottom of the cuvette. The average SAR over the whole sample normalized to 1 W input RF power was 50 ± 13 W.kg^{-1} (Table 1).

2.3 Numerical RF dosimetry - Numerical dosimetry was conducted using an in-house code based on the Finite Difference-Time Domain method (FDTD) applied to Maxwell equations [24-26]. The SAR distribution was computed using the equation:

$$SAR\left(W.kg^{-1}\right) = \sigma E^2/(2\rho) \qquad \textbf{(2)}$$

where E is the electric field (V/m), ρ is the biological sample density (1000 kg.m^{-3}) and σ is the electrical conductivity (S.m^{-1}). The TEM cell containing the cuvette filled with 3 ml water solution was modeled and analyzed. The metallic parts were considered perfect electric conductors. The cuvette permittivity was set to 3.7. The dielectric properties of the solution were: conductivity σ = 1.86 S/m, relative permittivity ε_r = 75.6 and mass density ρ = 1000 kg.m^{-3}. A uniform 0.2 mm × 0.2 mm × 0.2 mm mesh grid was used for the spatial meshing of the structure with the FDTD method.

Figure 1 (B) shows the numerical SAR spatial distribution within the cuvette solution and the SAR histogram at 1966 MHz. The mean SAR value and the standard deviation computed over the whole water solution medium were 47 ± 31 W.kg^{-1} per 1W input power. The mean SAR value can be compared to the experimental one (50 ± 13 W.kg^{-1}). A proper level of consistency was obtained between the numerical and the experimental SAR values.

2.4 Temperature control – Experiments were performed at the physiologic temperature of 37.0 ± 0.5 °C. To limit the temperature increase during RF exposure, the input power was attenuated down to 0.1 W. This generated an average SAR of 5.0 W.kg^{-1} in the sample. The temperature changes during the whole 60 min exposure period at 0.1 W input RF power was monitored at 4, 8, 16 and 24 mm heights from the bottom of the solution. The average maximum temperature elevation of the sample after 60 min exposure was 1.06°C.

Numerical temperature simulations were carried out using an explicit method based on finite difference applied to a heat transfer equation [27]:

$$\frac{\partial T}{\partial t} = \frac{1}{\rho C} div\left(k_t grad(T)\right) + \frac{P_c}{\rho C} \qquad \textbf{(3)}$$

where T is the temperature (K), ρ is the density (kg.m^{-3}), C is the specific heat capacity (J·K^{-1}·kg^{-1}), k_t is the thermal conductivity (W·m^{-1}·K^{-1}) and P_c is the calorific power inducing temperature elevation (W.m^{-3}). Due to the low temperature gradient, density is considered constant versus temperature and only thermal conduction was considered. The thermal characteristics used for the simulation are presented in Table 2.

2.5 SAR level in the experiments – The whole body SAR level for the most sensitive established health risk has been identified as 4 W.kg^{-1}. The proposed limit values for local exposures on the head have been defined as 2 W.kg^{-1} for public exposures and 10 W.kg^{-1} for occupational exposures. A target value of 5 W.kg^{-1} has been chosen to identify if adopted values are appropriate for people protection.

Figure 2 presents the numerical temperature rise for a 5 W.kg^{-1} mean SAR value. A temperature rise of about 1°C is observed after 1 hour of RF exposure. This value is consistent with the measured temperature rise (1.06°C).

2.6 Fluorescence spectroscopy - A Cary Eclipse Varian Australia spectrofluorimeter was used for the fluorescence experiments.

2.6.1) Tryptophan emission fluorescence

The excitation wavelength was adjusted to 295 nm, which was specific for the excitation of tryptophan (Trp) residues of the protein structure. Emission spectra were recorded between the wavelengths of 300 and 400 nm with a bandwidth of 10 nm. CPR samples were 130 nM of protein in a potassium phosphate buffer (100 mM, pH 7.0).

2.6.2) Flavin emission fluorescence

Flavin emission spectra were recorded from 475 to 600 nm using an excitation wavelength of 450 nm; 20-nm bandwidths were used for excitation and emission, respectively. CPR samples were 130 nM of protein in a potassium phosphate buffer (100 mM, pH 7.4).

2.7 Circular dichroism - CD spectra were obtained in the far-UV (260-199 nm) and visible range (350-600 nm) on a J-815 Jasco spectropolarimeter. The CD measurement was performed using a 10 mm-path cell, with 30 accumulations at a 130 nM concentration in 100 mM potassium phosphate buffer, pH 7.4. All CD spectra measured were baseline, corrected by subtracting the buffer spectrum. The secondary structure was determined by the CDNN 2.1. software, using a network trained with 33 complex spectra as the reference set.

2.8 Dynamic Light Scattering and microcapillary electrophoresis measurement - DLS is a technique for sizing particles using Brownian motion in conjunction with the Stokes-Einstein relationship assuming spherical particles. The hydrodynamic diameter and zeta potential of the sample were determined with a Malvern Zetasizer Nano-ZS, according to the manufacturer's recommendations. The instrument is equipped with a 633-nm He–Ne laser with 173° detection optics (backscatter detection). Protein samples (130 nM) were vortexed and transferred into either 1-ml glass cuvettes with round aperture or 1 ml clear zeta potential cuvettes (DTS1060, Malvern). The electrophoretic mobility of the sample was measured and converted into the zeta potential by applying the Henry equation [28]. The data were collected and analyzed with Dispersion Technology software 4.20 (Malvern) producing histograms for particle size as a number distribution or diagrams for the zeta potential as a distribution versus total counts.

2.9 Cytochrome C reductase activity - Protein activity can be regarded as the most sensitive probe for studying the changes in protein conformation during exposure, because it reflects even the subtlest readjustments at the active site. In this context, comparative CPR activities were measured via the reduction of cytochrome c, the surrogate electron acceptor most commonly used for measuring diflavin reductase activity [29]. All continuous spectrophotometric assays for CPR activity were performed using a total reaction volume of 1 ml in standard 1 cm quartz cuvettes. Experimental measurements were made on unexposed solutions and samples exposed for 1 hour at 5.0 $W.kg^{-1}$ SAR value to verify whether irradiation disturbs reaction mechanism. Cytochrome c reduction activity was measured as previously described [30] using different concentrations of cytochrome c (8.5-89 µM) and 100 µL of 130 nM of CPR in 900 µl of 300 mM potassium phosphate (pH 7.8). Increased absorbance at the wavelength of 550 nm followed after adding 250 µM NADPH. Cytochrome c reduction rates were calculated using ε_{550}=21 $mM^{-1}.cm^{-1}$ for reduced cytochrome c [31].

Results and discussion

3.1 Tryptophan fluorescence - Exposure of CPR to RF radiation resulted in a 10% decrease of intrinsic tryptophan fluorescence (Figure 3). Tryptophan emission fluorescence can be considered to be a sensitive marker of protein conformation and in particular of changes in hydrophobic regions of the structure [32]. Accordingly, a folded protein can have either greater or lesser fluorescence than the unfolded form. The intensity of fluorescence is not very informative in itself. The wavelength of the emitted light is a better indication of the environment of the fluorophore. The magnitude of intensity, however, can serve as an indication of perturbation to the folded state. The tryptophan fluorescence of the CPR comes from the 9 residues [33]. Thus, these changes in fluorescence reflect global changes in protein structure, and only the average microenvironments of tryptophan residues can be assessed. As exposure did not alter the overall shape of the fluorescence spectrum (no shift in the maximum, no spectrum enlargement), changes in the

fluorescence intensity at 335 nm were recorded. The absence of a shift clearly argues that the environment of most of the molecules is not significantly altered by the exposure to RF. The quenching of the tryptophan fluorescence could be explained in terms of emission energy transfer between the aromatic chromophore and the isoalloxazine ring [34, 35]. These results do suggest a need for further confirmation of the structural changes.

3.2 Flavin fluorescence - The fluorescence intensity of the two flavin prosthetic groups in the natural form of CPR is severely quenched by energy transfer to the surrounding protein matrix, rendering the detection of the fluorescence signal difficult. Figure 4 shows the flavin fluorescence spectra of unexposed and exposed CPR where the exposed protein showed enhancement of flavin fluorescence intensities. These changes in the fluorescence properties are likely to reflect the loss of protein-flavin contacts and probable changes in the tertiary structure of CPR (Munro and Noble 1999).

3.3 Circular dichroism (CD) spectroscopy - It is well known that far-UV CD and near-UV CD spectra are directly related, respectively, to the secondary structure and to the tertiary protein structure ([36], [37], [38]). To test whether the conformational transition monitored by fluorescence measurements reflected a disruption of the overall protein structure or was just indicative of local folding and to have a better knowledge of the structural properties at 5.0 $W.kg^{-1}$ SAR level, we analyzed RF induced modifications by CD spectroscopy. The secondary structure compositions (including α-helix, β-strand, turns and random coil) of these samples were calculated from their far-UV CD spectra according to the CDNN software program, as displayed in Figure 5. CD measures the difference in the absorbance of left versus right circularly polarized light and is therefore sensitive to the chirality of the environment. The far-UV CD spectrum provides quantifiable information about the secondary structure of a protein because each category of secondary structure (e.g., α-helix, β-sheet) has a different effect on the chiral environment of the peptide bond [39, 40]. The data indicate that RF exposure induced small but visible changes in the secondary structure of the protein (Table 3). The CD spectra experimental measurements, in the visible range (350-600 nm), were carried out in the same conditions than the far-UV. No difference in the tertiary structure was observed between the unexposed and the exposed protein solutions (data not shown).

3.4 Microcapillary electrophoresis and hydrodynamic diameters by dynamic light scattering - A prerequisite for the accurate determination of the dimensions of denatured proteins, as well as of the structural transitions they may undergo, is the ability to determine size parameters precisely and reproducibly. To confirm if observed changes in conformation of the CPR tend to change hydrodynamic diameters of the exposed sample, DLS measurements were made. Although CPR is asymmetrically shaped in its natural conformation, DLS can provide a relative measurement of protein size, which can be used to discriminate between different conformational states. A shift in the zeta potential is observed at pH 7.0 (originally negative, then positive after exposure), indicating that the total surface charge at the sliding plane becomes, as a mean value, more positive in the exposed sample (data not shown). Perhaps, the topological distribution of charges and their interaction with electromagnetic fields can cause a conformational modification. The average hydrodynamic diameter was decreased in the exposed sample (10±3) compared to the unexposed one (15±2) to (Figure 6). These findings are consistent with the behavior observed with fluorescence and CD spectroscopy and represent further evidence of the occurrence of conformational changes in the exposed sample. It has been demonstrated that a correlation exists between the relative decrease in hydrodynamic radii and the increase in secondary structure content [41].

3.5 Cytochrome C reductase activity - Figure 7 shows the Lineaweaver-Burk plots; the kinetic parameters Km and Vmax were calculated from the intercept and the slope of the linear fit. The Lineweaver-Burk equation is:

$$\frac{1}{V} = \frac{K_m}{V_{\max}}[S]^{-1} + \frac{1}{V_{\max}} \quad \textbf{(4)}$$

where V is the reaction velocity ($mM.min^{-1}$), $[S]$ the substrate concentration (mM), K_m is the Michaelis–Menten constant (mM), V_{max} is the maximum reaction velocity ($mM.min^{-1}$). From measurement, we obtain V^{-1}=3.05 (±0.09) $[S]^{-1}$+77.2 (±3.3) $mM^{-1}.min$ for the sham-exposed condition and V^{-1}=3.1

(±0.10) $[S]^{-1}$+98.5 (±3.6) mM^{-1}.min for the exposed condition. The RF exposure produced a 22% decrease in both Km and Vmax as compared with control values. The inhibition pattern appears to be uncompetitive inhibition; the enzyme's apparent affinity for the substrate is increased (Km is lowered) which decreases the maximum enzyme activity (Vmax), as it takes longer for the substrate or product to leave the active site [42]. This decrease in enzyme activity can be indirectly related to the electron transfer ability upon alteration of the structure of cytochrome P450 reductase under WCDMA modulated RF exposure.

3.6 Role of temperature increase - The observed effects could be due to the increase in temperature produced by the absorption of electromagnetic energy (dielectric absorption). To test this hypothesis, a complementary experiment was performed to compare the fluorescence spectra of flavin exposed for one hour to 1966 MHz-RF and placed at 40°C for one hour. The increase in intensity was much lower at 40°C (-10 fluorescence units) than after a one-hour exposure to RF producing a 1°C-Temperature increase, i.e. 38°C (-30 fluorescence units), indicating that the shift produced by RF was not exclusively due to temperature (Figure 8).

Conclusion and perspectives

Spectroscopic, microelectrophoretic and DLS data have demonstrated that exposure to RF of 3G mobile telephone systems can induce some structural changes in CPR. The far UV CD spectra gathered in the peptide absorption range show that exposure affects the secondary structure of the enzyme, whilst evidence of tertiary structure modification is revealed by the change of tryptophan and flavin fluorescence intensity. This clearly shows that the interaction of RF energy gives the protein a conformation that is naturally irreversible, providing a clear modification of kinetic parameters. It will be of interest to look further into whether this biological effect brought about by this exposure level of 3G-RF could potentially be associated with adverse health effects. The relevance of these findings to real RF exposure scenarios, however, demands further biochemical and in vivo confirmation. A SAR of 5.0 $W.kg^{-1}$ is larger than a realistic SAR produced by commercial phones, limited by standards at a maximum of 2.0 $W.kg^{-1}$, but just above the identified health risk level of 4 $W.kg^{-1}$ for whole body exposure. It will then be important to further define exposure levels and durations that can result in changes in protein conformation and activity. It is also quite possible that the effects of RF radiation in fully integrated biological systems may either be masked by repair and regulation mechanisms or be transient. Thus, to systematically detect RF influences, a bottom-up approach is suggested, by reconstituting the complex system from individual enzymes, for example CPR and one of the isoforms of the microsomal cytochrome P450. This two protein membrane enzyme complex could be a suitable model for further investigation as it catalyzes the transformation of a number of xenobiotic substrates.

A better knowledge of interactions between RF exposure and molecules will possibly help to understand the mechanisms for these effects, and the health consequences for humans.

Acknowledgments

This work was supported by the "Fondation UTC pour l'Innovation – Programme Toxicologie Ecotoxicologie" and INERIS. The authors thank Caroline Gourland for editing the references under the Bioelectrochemistry style.

Conflict of interest

The authors declare that they have no conflicts of interest with the contents of this article.

Author contributions

ST conceived the study, performed fluorescence spectroscopy, DLS, microelectrophoresis and biochemical analyses (Figures 4, 5, 7, 8, 9, 10) and wrote the paper. GT checked the exposure system, conceived and analyzed the experimental dosimetry. BS and RDS coordinated the study. VSPA and PS designed, performed and analyzed the CD experiments shown in Figure 6. PL and DAC designed, performed and analyzed the exposure setup shown in Figure 1 and modeled the numerical dosimetry shown in Figures 2 and 3. They also provided technical assistance and contributed to the preparation of the figures. SP supervised the work and contributed substantially to the writing of the paper. All authors reviewed the results and approved the final version of the manuscript.

References

1. Desai, N.R., K.K. Kesari, and A. Agarwal, *Pathophysiology of cell phone radiation: oxidative stress and carcinogenesis with focus on male reproductive system.* Reproductive Biology and Endocrinology, 2009. **7**.
2. Karinen, A., et al., *Mobile phone radiation might alter protein expression in human skin.* Bmc Genomics, 2008. **9**.
3. Mousavy, S.J., et al., *Effects of mobile phone radiofrequency on the structure and function of the normal human hemoglobin.* International Journal of Biological Macromolecules, 2009. **44**(3): p. 278-285.
4. Bismuto, E., et al., *Are the conformational dynamics and the ligand binding properties of myoglobin affected by exposure to microwave radiation?* European Biophysics Journal with Biophysics Letters, 2003. **32**(7): p. 628-634.
5. Blank, M., *Protein and DNA reactions stimulated by electromagnetic fields.* Electromagnetic Biology and Medicine, 2008. **27**(1): p. 3-23.
6. Mancinelli, F., et al., *Non-thermal effects of electromagnetic fields at mobile phone frequency on the refolding of an intracellular protein: myoglobin.* Journal of Cellular Biochemistry, 2004. **93**(1): p. 188-196.
7. Reed, J.R. and W.L. Backes, *Formation of P450 . P450 complexes and their effect on P450 function.* Pharmacology & Therapeutics, 2012. **133**(3): p. 299-310.
8. Munro, A. and M. Noble, *Fluorescence analysis of flavoproteins*, in *Flavoprotein Protocols*, S. Chapman and G. Reid, Editors. 1999, Humana Press. p. 25-48.
9. Wang, M., et al., *Three-dimensional structure of NADPH-cytochrome P450 reductase: Prototype for FMN- and FAD-containing enzymes.* Proceedings of the National Academy of Sciences of the United States of America, 1997. **94**: p. 8411-8416.
10. Shen, A.L. and C.B. Kasper, in *Handbook of Experimental Pharmacology*. 1993, Springer-VErlag: New York. p. 35-59.
11. Strobel, H., A. Hodgson, and S. Shen, *Cytochrome P150: structure, mechanism, and biochemistry*, P.R. Ortiz, Editor. 1995, PlenumPress: New York and London. p. 225-244.
12. Phillips, A.H. and R.G. Langdon, *Hepatic triphosphopyridine nucleotide-cytochrome C reductase - Isolation, characterization, and kinetic studies.* Journal of Biological Chemistry, 1962. **237**(8): p. 2652-2660.
13. Williams, C.H. and H. Kamin, *Microsomal triphosphopyridine nucleotide-cytochrome C reductase of liver.* Journal of Biological Chemistry, 1962. **237**(2): p. 587-595.
14. Schacter, B.A., et al., *Immunochemical evidence for an association of heme oxygenase with the microsomal electron-transport system.* Journal of Biological Chemistry, 1972. **247**(11): p. 3601-3607.
15. Enoch, H.G. and P. Strittmatter, *Cytochrome-B5 reduction by NADPH-cytochrome P-450 reductase.* Journal of Biological Chemistry, 1979. **254**(18): p. 8976-8981.
16. Horecker, B.L., *Triphosphopyridine nucleotide-cytochrome-C reductase in liver.* Journal of Biological Chemistry, 1950. **183**(2): p. 593-605.
17. Corbett, J.C.W. and R.O. Jack, *Measuring protein mobility using modern microelectrophoresis.* Colloids and Surfaces a-Physicochemical and Engineering Aspects, 2011. **376**(1-3): p. 31-41.

18. Jachimska, B. and A. Pajor, *Physico-chemical characterization of bovine serum albumin in solution and as deposited on surfaces.* Bioelectrochemistry, 2012. **87**: p. 138-146.
19. Thielbeer, F., K. Donaldson, and M. Bradley, *Zeta potential mediated reaction monitoring on nano and microparticles.* Bioconjugate Chemistry, 2011. **22**(2): p. 144-150.
20. Jarrige, P., et al., *Electrooptic probe adapted for bioelectromagnetic experimental investigations.* Instrumentation and Measurement, IEEE Transactions on, 2012. **61**(7): p. 2051-2058.
21. Kohler, S., et al., *Setup for simultaneous microwave heating and real-time spectrofluorometric measurements in biological systems.* Progress in Electromagnetics Research, 2014. **145**: p. 229-240.
22. O'Connor, R.P., et al., *Exposure to GSM RF fields does not affect calcium homeostasis in human endothelial cells, rat pheocromocytoma cells or rat hippocampal neurons.* Plos One, 2010. **5**(7).
23. Ticaud, N., et al., *Specific absorption rate assessment using simultaneous electric field and temperature measurements.* Antennas and Wireless Propagation Letters, IEEE, 2012. **11**: p. 252-255.
24. Leveque, P., A. Reineix, and B. Jecko, *Modeling of dielectric losses in microstrip patch antennas - application of FDTD method.* Electronics Letters, 1992. **28**(6): p. 539-541.
25. Taflove, A. and S.C. Hagness, *Computational electrodynamics : the finite-difference time-domain method*. 3rd ed. 2005, Boston: Artech House. xxii, 1006.
26. Yee, K., *Numerical solution of initial boundary value problems involving maxwell's equations in isotropic media.* Antennas and Propagation, IEEE Transactions on, 1966. **14**(3): p. 302-307.
27. Cueille, M., et al., *Development of a numerical model connecting electromagnetism, thermal and hydrodynamics to analyse in vitro exposure system.* Annales Des Telecommunications-Annals of Telecommunications, 2008. **63**(1-2): p. 17-28.
28. Adak, S., S. Chowdhury, and M. Bhattacharyya, *Dynamic and electrokinetic behavior of erythrocyte membrane in diabetes mellitus and diabetic cardiovascular disease.* Biochimica Et Biophysica Acta-General Subjects, 2008. **1780**(2): p. 108-115.
29. Lian, L.Y., et al., *Biochemical comparison of anopheles gambiae and human NADPH P450 reductases reveals different 2 '-5 '-ADP and FMN binding traits.* Plos One, 2011. **6**(5).
30. Shen, A.L. and C.B. Kasper, *Role of acidic residues in the interaction of NADPH-cytochrome-P450 oxidoreductase with cytochrome-P450 and cytochrome-C.* Journal of Biological Chemistry, 1995. **270**(46): p. 27475-27480.
31. Vermilion, J.L., et al., *Separate roles for FMN and FAD in catalysis by liver microsomal NADPH-cytochrome P-450 reductase.* Journal of Biological Chemistry, 1981. **256**(1): p. 266-277.
32. Royer, C.A., *Probing protein folding and conformational transitions with fluorescence.* Chemical Reviews, 2006. **106**(5): p. 1769-1784.
33. Yamano, S., et al., *Human NADPH-P450 oxidoreductase - Complementary-DNA cloning, sequence and vaccinia virus-mediated expression and localization of the CYPOR gene to chromosome-7.* Molecular Pharmacology, 1989. **36**(1): p. 83-88.
34. Haouz, A., et al., *Forster energy transfer from tryptophan to flavin in glucose oxidase enzyme.* Chemical Physics Letters, 1998. **294**(1-3): p. 197-203.

35. Nisimoto, Y. and Y. Shibata, *Studies on FAD- and FMN-binding domains in NADPH-cytochrome-P-450 reductase from rabbit liver-microsomes.* Journal of Biological Chemistry, 1982. **257**(21): p. 12532-12539.
36. Zhu, Y., G. Cheng, and S. Dong, *The electrochemically induced conformational transition of disulfides in bovine serum albumin studied by thin layer circular dichroism spectroelectrochemistry*. Biophysical Chemistry, 2001. **90**: p. 1-8.
37. Tetin, S.Y., F.G. Prendergast, and S. Yu, *Accuracy of protein secondary structure determination from circular dichroism spectra based on immunoglobulin examples.* Analytical Biochemistry, 2003. **321**: p. 183-187.
38. Azimi, O., et al., *Probing the Interaction of Human Serum Albumin with Norfloxacin in the Presence of High-Frequency Electromagnetic Fields: Fluorescence Spectroscopy and Circular Dichroism Investigations.* Molecules 2011. **16**: p. 9792-9818.
39. Greenfield, N., *Circular dichroism analysis for protein-protein interactions*, in *Protein-Protein Interactions*, H. Fu, Editor. 2004, Humana Press. p. 55-77.
40. Kaminsky, J., J. Kubelka, and P. Bour, *Theoretical modeling of peptide alpha-helical circular dichroism in aqueous solution.* Journal of Physical Chemistry A, 2011. **115**(9): p. 1734-1742.
41. Uversky, V.N. and A.L. Fink, *The chicken-egg scenario of protein folding revisited.* Febs Letters, 2002. **515**(1-3): p. 79-83.
42. Purich, D.L., *Chapter 8 - Kinetic behavior of enzyme inhibitors*, in *Enzyme Kinetics: Catalysis & Control*, D.L. Purich, Editor. 2010, Elsevier: Boston. p. 485-574.

Vitae

Shazia Tanvir holds a PhD degree in Enzyme and Cell Engineering and two Masters in Biotechnology and Microbiology. She completed two postdoctoral fellowships funded by Université de Technologie de Compiègne (France) and University of Waterloo (Canada). Shazia is working at Genemis Laboratories (Ontario) as a Chief Scientific Officer. She also provides a broad range of consultation services to infection control industries in Ontario. She holds the honor of being a reviewer in the most prestigious scientific journals of her discipline.

Dr.Thuróczy received the M.Sc. Degree in electrical engineering from the Technical University of Budapest in 1983. He received the doctoral degree in biophysics from the Institute of Biophysics of Medical University of Budapest and Ph.D. degree of neurobiology from University of Pécs, Hungary. Now he is the head of Department of Non-Ionizing Radiation He is the member of International Advisory Committee of WHO EMF Project, member of Management Committee of COST BM1309, member of International Committee of Electromagnetic Safety (ICES) and member of the Bioelectromagnetics Society (BEMS), He is the national representatives of EU and international Standard Committees (CENELEC, IEC).

Brahim SELMAOUI received a Master of Biochemistry and a Ph.D. in endocrinology. He received a scholarship of excellence from the government of Quebec which allowed him to pursue a post doctoral position at Mc Gill University. He also worked as research scientist in the laboratory of chronobiology (Montreal). He then joined the department of immunotoxicology at Charles River Laboratories (Canada) where he was appointed as scientist. Currently, he is working in the department of toxicology as senior scientist at INERIS. He is serving as an expert reviewer for more than 4 different scientific and medical journals, granting agency and WHO.

Viviane Silva Pires-Antonietti was born in Porto Alegre, Brazil, in 1973. She received a Master in Pharmaceutics Science in 2001 from the Federal University of Rio Grande do Sul, Brazil. In 2006, she received a Ph.D degree in Chemistry from the University of Picardie Jules Verne (UPJV), France. She joined the Faculty of Pharmacy, UPJV, France as an Assistant Professor in Pharmaceutical technology in 2007. Her current researches concern the design and development of iron chelators and antibacterial drugs.

Pascal Sonnet received his Ph.D. degree in Medicinal Chemistry from Caen University (1997). He performed his postdoctoral training as a Postdoctoral Research Assistant in the Synthetic Organic Chemistry Charette's Group, University of Montreal, Canada, from 1997 to 1998. He joined the Faculty of Pharmacy, University of Picardie Jules Verne, Amiens as an Assistant Professor in Medicinal Chemistry in 1998, then was promoted to Professor in 2004. His research interests concern the design and development of iron chelators, antibacterial, and antimalarial drugs.

Delia Arnaud-Cormos was born in Cugir, Romania, in 1978. She received the master's and Ph.D. degrees from the National Institute of Applied Sciences, Rennes, in 2003 and 2006, respectively. She joined the Xlim Institute, CNRS, University of Limoges, France, in 2007, as an Associate Professor. In 2012, she joined the Pulsed Power Group with the Department of Electrical Engineering, University of Southern California, Los Angeles, CA, USA, where she developed research with team led by Dr. P.T. Vernier. Her current research interests include nanosecond pulses/microwave exposure systems setup and dosimetric characterization for bioelectromagnetics studies.

Philippe Leveque was born in Poitiers, France, in 1964. He received the Ph.D. degree from the University of Limoges, France, in 1994. He joined the Centre National de la Recherche Scientifique (CNRS) in 1995. He is involved in the dosimetry and development of exposure setups for therapeutic application and health-risk assessment in cooperation with biological and medical research groups. He is currently the

CNRS senior researcher and the leader of Bioelectrophotonics group at the XLIM research institute, where he is involved in bioelectromagnetism and nanosecond pulse electric field application.

Sylviane Pulvin obtained a PhD in Industrial Process Engineering from Compiègne University of Technology, France, in 1979. She then prepared a Habilitation thesis on the stability of enzyme systems with gaseous substrates or products, which she defended in 1991 at the same university. She has been holding positions as teaching and research assistant and associate professor at Compiègne University of Technology, between 1974 and 2005, before becoming a full Professor in Bioengineering in 2005. Her research interests include homogeneous and heterogeneous enzymatic catalysis, organic synthesis, affinity technology and protein purification, biosensors, and biomimicry.

René de Seze is radiologist MD, with a Masters in physics, a PhD in life sciences and a ducent. He worked in Radiology and Biophysics at Montpellier University, and is now Senior Researcher at INERIS, the research institute of the ecology Ministry. After 27 papers and 130 meeting communications in therapeutics, exposure systems and biological effects, specifically in human volunteers, his research focused on the health effects of cellular telephony radiowaves. He served as secretary or President of national (SFRP-NIR), European (EBEA) and international (BEMS) organizations working in bioelectromagnetics, and as expert in several groups (ANSES, ICNIRP, WHO, …).

Figure legends

Schematic 1. In vitro exposure system with a TEM cell connected to a UMTS signal generator and RF amplifier housed in the incubator.

Figure 1. (A) Numerical modeling of SAR spatial distribution within the cuvette solution and (B) SAR histogram at 1966 MHz with 1 W input power. N_{count} represents the number of voxels as a function of the specific absorption rate values (SAR/W.kg^{-1}).

Figure 2. Average temperature rise (T/°C) as a function of time (t/min) for 5 W.kg^{-1} mean SAR value obtained from numerical simulations of the sample.

Figure 3. Tryptophan fluorescence intensity (FI/a.u.) as a function of wavelength (λ/nm) corresponding to the emission spectra of CPR in 100 mM potassium phosphate buffer (pH 7). Unexposed (—) and exposed (- - -) proteins at 5 W.kg^{-1} of specific absorption rate. Experimental conditions: CPR [130 nM] excitation wave length 295 nm.

Figure 4. Flavin fluorescence intensity (FI/a.u.) as a function of wavelength (λ/nm) corresponding to the emission spectra of CPR samples in 100 mM potassium phosphate buffer (pH 7.4). Unexposed (—) and exposed (- - -) proteins at 5 W.kg^{-1} of specific absorption rate. Experimental conditions: CPR [130 nM] excitation wave length 450 nm.

Figure 5. Far-UV CD spectra, circular dichroism (CD/mdeg) as a function of wavelength (λ/nm), of CPR samples in 100 mM potassium phosphate buffer (pH 7.4). Unexposed (—) and exposed (- - -) proteins at 5 W.kg^{-1} of specific absorption rate. Experimental conditions: CPR [130 nM].

Figure 6. Particle distribution (PD/%) histograms as a function of hydrodynamic diameter (ø/nm) measured by DLS recorded in 100 mM potassium phosphate buffer (pH 7.4). Unexposed (light gray) and exposed (dark gray) proteins at 5 W.kg^{-1} of specific absorption rate. Experimental conditions: CPR [130 nM].

Figure 7. Reaction velocity (V^{-1}/min.mM^{-1}) as a function of cytochrome P450 reductase substrate ([S] $^{-1}$/mM^{-1}): Lineweaver-Burk plot of cytochrome P450 reductase samples after 1 hour exposure to RF 1966 MHz (130 nM, pH 7.8, 100 mM potassium phosphate buffer). Unexposed (—) and exposed (- - -) proteins at 5 W.kg^{-1} of specific absorption rate. Reduction of cytochrome C measured spectrophotometrically by recording the absorbance at 550 nm.

Figure 8. Flavin fluorescence intensity (FI/a.u.) as a function of wavelength (λ/nm). Unexposed at 37°C (—), unexposed at 40°C (⋯), and exposed (- - -) proteins at 5 W.kg^{-1} of specific absorption rate. Comparison of the fluorescence shift of flavin produced by a 3°C increase by conventional warming at 40°C and by the 1°C increase by RF absorption at 5 W.kg^{-1}.

Tables

Height (mm)	dT* (^oC)	SAR* ($W.kg^{-1}$)	N-SAR ($(W.kg^{-1}).W^{-1}$)
4	0.82	114	29.3
8	1.17	163	41.9
12	1.38	192	49.5
16	1.71	234	61.3
20	1.79	250	64.4
24	1.52	212	54.7

*at 3.88 W RF input power

Table 1. Temperature elevation and SAR[2] at different heights in the sample, taken from the bottom of the cuvette. Normalized SAR at 1 W input power (N-SAR) is also calculated.

	Air	Solution	Plastic	Stainless steel
k_t ($W \cdot m^{-1} \cdot K^{-1}$)	0.025	0.606	0.12	1.6
C ($J \cdot K^{-1} \cdot kg^{-1}$)	1012	4178	1400	500
ρ ($kg.m^{-3}$)	1.16	1000	1100	7900

Table 2. Thermal properties of each element used for simulations.

	Unexposed (mdeg) 200-260 nm (%)	**Exposed (mdeg)** 200-260 nm (%)
Helix	57.2	50.2
Antiparallel	9.3	8.8
Parallel	7.8	6.8
Beta-Turn	7.6	9.6
Random Coil	22.3	23.4

Table 3. Secondary structure compositions of CPR at pH 7.4 (100 mM, potassium phosphate buffer) as calculated from far-UV CD spectra by the CDNN 2.1. software.

[2] SAR: specific absorption rate; k_t: thermal conductivity; C: heat capacity; ρ: volumetric weight

Figures

Schematic 1

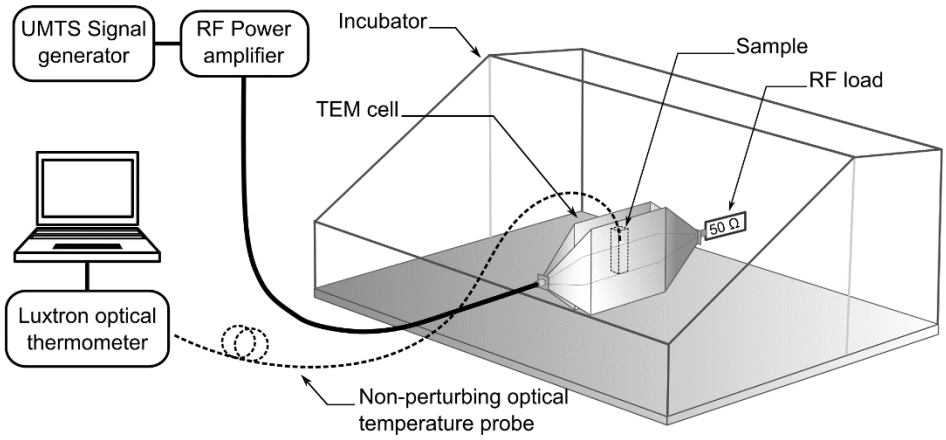

Figure 1

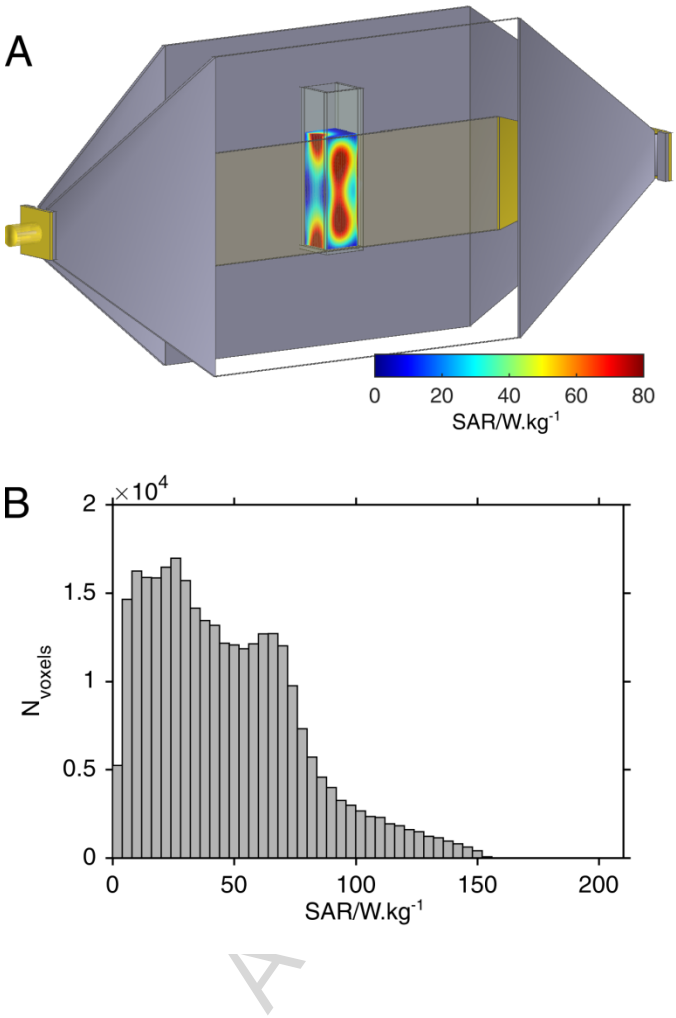

Figure 2

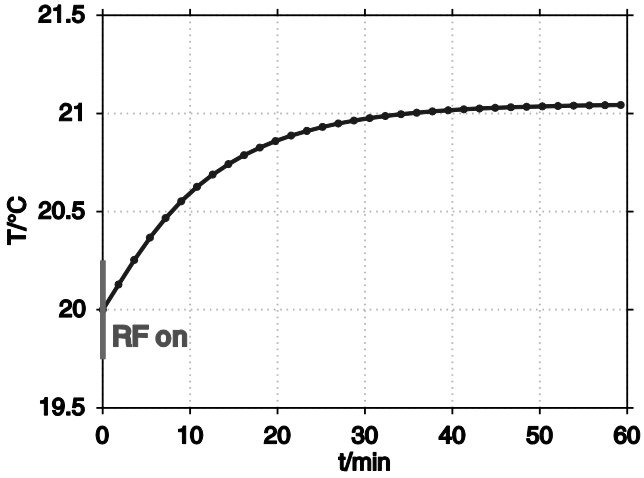

Figure 3

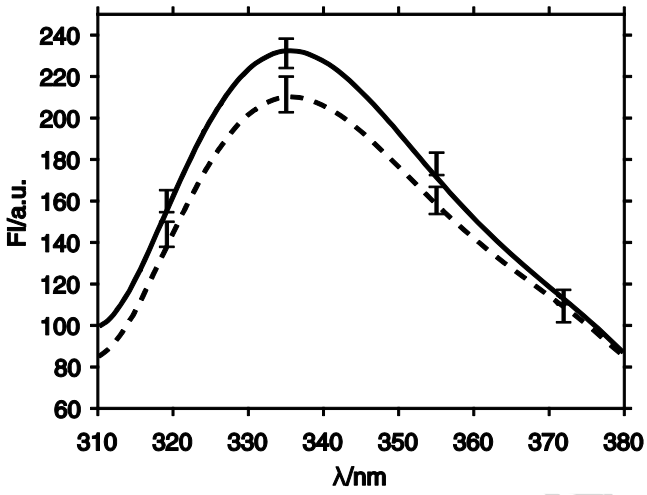

Figure 4

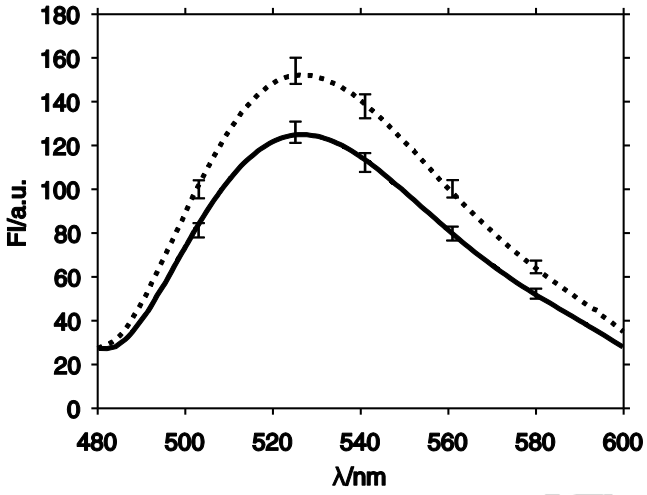

Figure 5

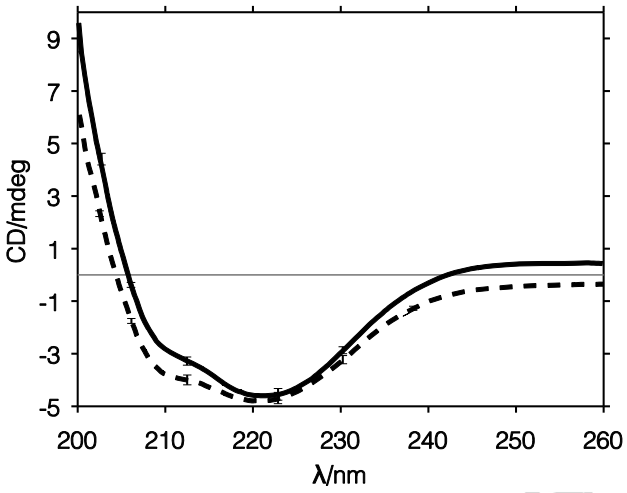

Figure 6

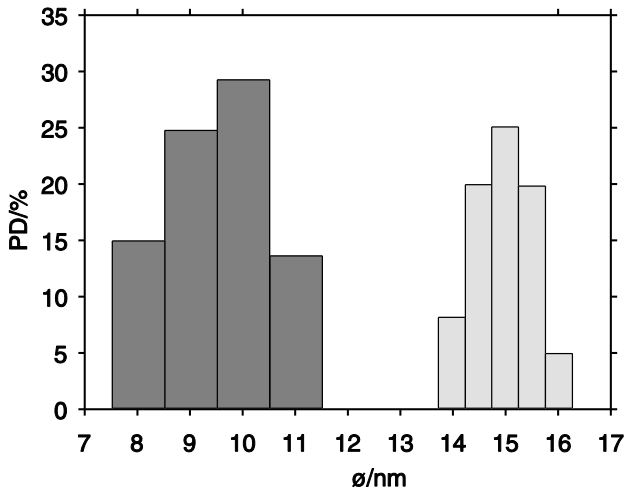

Figure 7

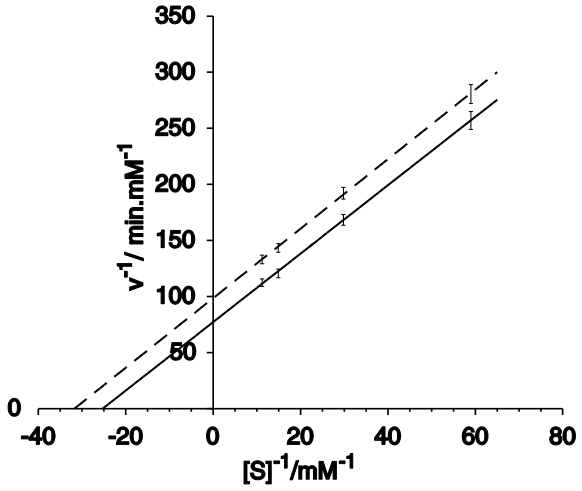

Figure 8

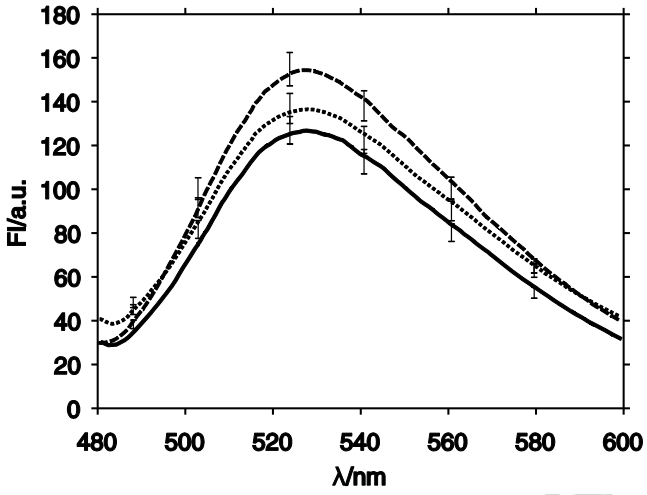

Authors' photographs

Shazia Tanvir

György Thuróczy

Brahim Selmaoui

Viviane Silva Pires-Antonietti

Pascal Sonnet

Delia Arnaud-Cormos

Philippe Lévêque

Sylviane Pulvin

René de Seze

Graphical Abstract

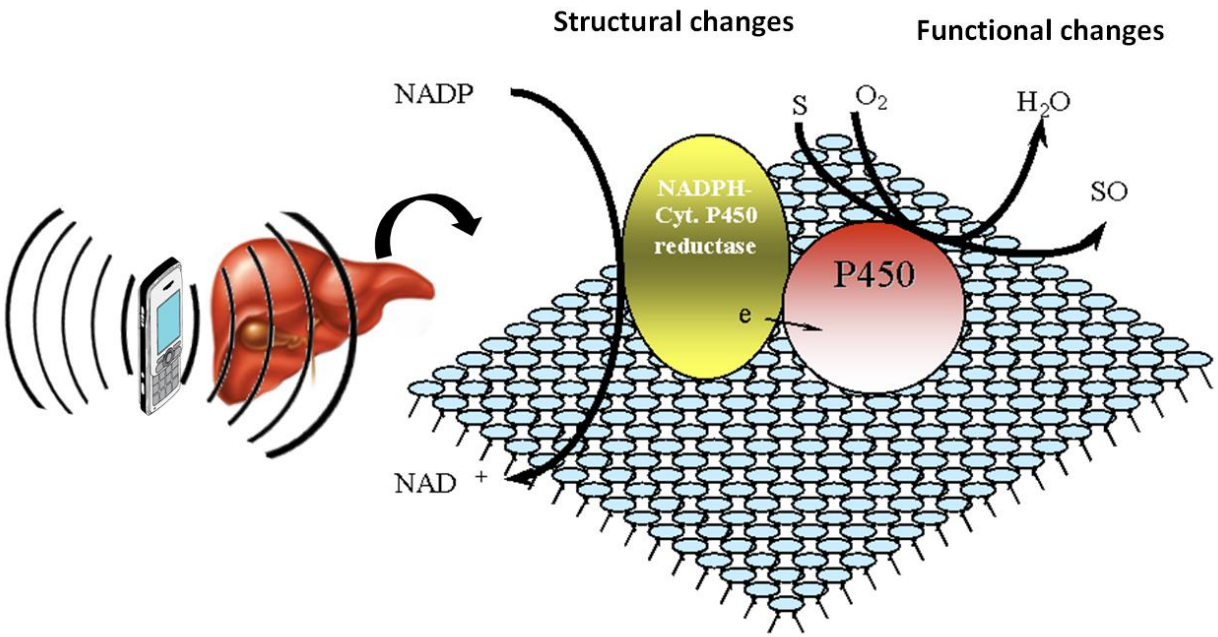

Highlights

Structure of cytochrome P450 reductase was altered under mobile phone-like exposure.
Circular dichroism and dynamic light scattering showed protein conformation narrowing.
Activity assessed by reduction of cytochrome c was decreased.
Heating alone does not explain this effect, meaning that its mechanism must be sought.
If this happens at usage power, it could alter detoxification metabolism in humans.